J Appl Electrochem (2013) 43:611–617
DOI 10.1007/s10800-013-0542-5

ORIGINAL PAPER

Chemical lithiation route to size-controllable $LiFePO_4$/C nanocomposite

Yong Jiang · Hua Zhuang · Dengyu Pan · Zheng Jiao · Xiaochao Que · Xuetao Ling · Mingyang Zhong · Yuliang Chu · Bing Zhao

Received: 17 January 2013 / Accepted: 4 April 2013 / Published online: 18 April 2013

Abstract Chemical lithiation of amorphous $FePO_4$ with LiI in acetonitrile is performed to form amorphous $LiFePO_4$. The amorphous $FePO_4{\cdot}2H_2O$ precursor is synthesized by co-precipitation method from equimolar aqueous solutions of $FeSO_4{\cdot}7H_2O$ and $NH_4H_2PO_4$, using H_2O_2 (hydrogen peroxide) as the oxidizing agent. The nanocrystalline $LiFePO_4$/C is obtained by annealing the amorphous $LiFePO_4$ and in situ carbon coating with sucrose in a reducing atmosphere. The particle size of $FePO_4{\cdot}2H_2O$ precursor decreases with increasing reaction temperature. The final $LiFePO_4$/C products completely maintain the shape and size of the precursor even after annealing at 700 °C for 2 h. The excellent electrochemical properties of these nanocrystalline $LiFePO_4$/C composites suggest that to decrease the particle size of $LiFePO_4$ is very effective in enhancing the rate capability and cycle performance. The specific discharge capacities of $LiFePO_4$/C obtained from the $FePO_4{\cdot}2H_2O$ precursor synthesized at 75 °C are 151.8 and 133.5 mAh g^{-1} at 0.1 and 1 C rates, with a low capacity fading of about 0.075 % per cycle over 50 cycles at 0.5 C rate.

Keywords Iron phosphate · $LiFePO_4$/C composite · Chemical lithiation · Size-controllable · Electrochemical performance

Y. Jiang · H. Zhuang · D. Pan · Z. Jiao · X. Que · X. Ling · M. Zhong · B. Zhao (✉)
School of Environmental and Chemical Engineering, Shanghai University, Shanghai 200444, People's Republic of China
e-mail: bzhao@shu.edu.cn

Y. Chu
Instrumental Analysis and Research Center, Shanghai University, Shanghai 200444, People's Republic of China

1 Introduction

Olivine-type $LiFePO_4$, reported by the Goodenough group in 1997 [1], has received great attention because of its low cost, good capacity retention and improved safety [2]. These properties make it an attractive candidate for large batteries, which are required for electric and hybrid electric vehicles [3].

The power capability of this material is limited by its low electronic conductivity ($\sim 10^{-9}$ S cm^{-2}) and Li^+ diffusion rate [4]. To improve the electronic conductivity, many attempts such as cation-doping [5, 6], carbon-coating [7, 8], anion-doping [9], and particle-size controlling [10] have been directed to overcome the drawback of $LiFePO_4$. Among them, water-phase reactions and carbon-coating are effective to control its particle size and improve its conductivity [11–13]. However, it's hard to synthesize pure olivine $LiFePO_4$ through aqueous reactions, which inevitably introduce Fe^{3+} impurity in final products [14, 15].

More recently, it has been widely reported that $LiFePO_4$/C can be synthesized through carbothermal reduction of $FePO_4$ [11, 16, 17]. This composite is expected to exhibit high tap density. However, its electrochemical properties disappoint us usually because of its large size and serious agglomeration [18]. It is known that lithium diffusion through diminishing $LiFePO_4/FePO_4$ interface limits the rate performance of $LiFePO_4$ material. According to the Radial Model [19], the surface area of $FePO_4$ decreases during the deintercalation process and the amount of lithium passing through the interface is insufficient to sustain the current, leading to a decrease in reversible capacity at higher current densities. More lithium can be extracted and reinserted reversibly in samples composed of smaller grains [20]. Therefore, in situ polymerization restriction methods for the synthesis of $LiFePO_4$/carbon nanocomposites were reported from $FePO_4$/polymer precursors

(such as polyaniline [21], stearic acid [22], and vinyl polymers [23]). However, little has been reported on the effects of synthetic procedures such as reaction temperature, pH, and concentrations of precursors on the particle size and morphology of $FePO_4$ and $LiFePO_4$.

In this study, size-controllable $FePO_4{\cdot}2H_2O$ nanoparticles were synthesized at different temperatures by co-precipitation method. Then the precursor was lithiated by using LiI in acetonitrile as a reducing agent and a lithium source. Chemical lithiation owns the advantages of (i) guaranteeing the homogeneous distribution of atomic scale for all the components, (ii) thus allowing a reduction of heating temperature and sintering time, (iii) moreover, avoiding either low discharge capacity or large capacity fading due to the presence of impurity phases and low crystallinity in the prepared materials [24–27]. In this study, we explored the optimal conditions to obtain highly crystalline olivine $LiFePO_4$/C and employed thermogravimeter (TG), X-ray diffraction (XRD), and scanning electronic microscope (SEM) to characterize its composition, structure, and morphology. The electrochemical property of the composite was also evaluated.

2 Experimental

2.1 Synthesis of $FePO_4{\cdot}2H_2O$

Amorphous $FePO_4{\cdot}2H_2O$ was synthesized by a co-precipitation method. An aqueous solution of 0.01 M $NH_4H_2PO_4$ was slowly added to an equivolume solution of 0.01 M $FeSO_4{\cdot}7H_2O$ under stirring. Then diluted H_2O_2 solution (0.94 wt%, 10 mL) was added at controlled dropping rates to the mixed solution at different temperatures (0, 25, 50, 75 °C) under vigorous stirring. The molar ratio of H_2O_2 to $FeSO_4{\cdot}7H_2O$ was 0.55:1. Yellow $FePO_4{\cdot}2H_2O$ precipitate formed immediately after adding H_2O_2. After stirring for 2 h, the precipitate was washed several times with distilled water and separated by centrifugation, then dried in oven at 80 °C overnight.

2.2 Synthesis of $LiFePO_4$/C

To prepare $LiFePO_4$, the chemical lithiation of the amorphous $FePO_4$ was performed with LiI as a reducing agent and lithium source [26]. Firstly, $FePO_4{\cdot}2H_2O$ was annealed in air at 400 °C for 6 h to eliminate crystalline water. Then the amorphous anhydrous $FePO_4$ was suspended in a 0.5 M solution of LiI in acetonitrile (Li/Fe = 3/1 mol ratio). Superfluous LiI was used to completely reduce Fe^{3+} in $FePO_4$ to Fe^{2+}. The suspension was constantly stirred for 24 h at ambient temperature. After that the precipitate was washed several times with acetonitrile to remove remaining LiI, separated by centrifugation and dried under vacuum at 60 °C for 2 h. Note that the chemical lithiation was performed in an Ar-filled glove box because of the hygroscopic nature of LiI. To obtain carbon-coated $LiFePO_4$, the lithiation compound was mixed equably with sucrose in ethanol, and then calcined at 700 °C for 2 h under reducing atmosphere ($Ar/H_2 = 95/5$) with a heating rate of 5 °C min^{-1}.

2.3 Characterization of synthesized $FePO_4$ and $LiFePO_4$/C

The phase structures of the powders were analyzed by XRD on a Rigaku-D/MAX-2550PC diffractometer with Cu Kα radiation at a 2θ step size of 0.02°. The elemental analysis of the precipitate (Li, Fe, P) was performed by flame and graphite atomic absorption spectrometries (Varian 220FS). The powder morphology was observed by JEOL JSM-6700F (FESEM). A thermogravimetry–differential thermal analysis (TG–DTA) apparatus Germany Netzsch-STA409PC instrument was used for the thermal characterization.

2.4 Electrode fabrication and electrochemical measurements

The electrochemical properties of the $LiFePO_4$/C powders were studied by assembling 2016 coin cells with lithium metal as an anode and 1 M $LiPF_6$ in dimethyl carbonate, diethyl carbonate, and ethylene carbonate (1:1:1 by weight) as electrolyte. Constant current during cell cycling was set to a value between 17 and 850 mA g^{-1} (i.e. between 0.1 and 5 C). Cyclic voltammograms (CV) were recorded using a lithium foil as both counter and reference electrodes with a scan rate of 0.1 mV s^{-1} between 2.5 and 4.2 V.

3 Results and discussion

The $FePO_4$ precursor was synthesized by co-precipitation from $FeSO_4{\cdot}7H_2O$ and $NH_4H_2PO_4$ using H_2O_2 as the oxidizing agent. The reaction equation was as follows:

$$2FeSO_4 + 2NH_4H_2PO_4 + H_2O_2 + 2H_2O \rightarrow 2FePO_4 \cdot 2H_2O + 2NH_4HSO_4$$

The TG–DTA curves of the $FePO_4$ precipitate are shown in Fig. 1. In the temperature range from room-temperature to 400 °C, there is a continuous weight loss in the TG curve, corresponding to the elimination of water. In the first stage from room temperature to ~162 °C, about 9.4 % weight loss is related to the loss of 1.0 mol of water per mol of

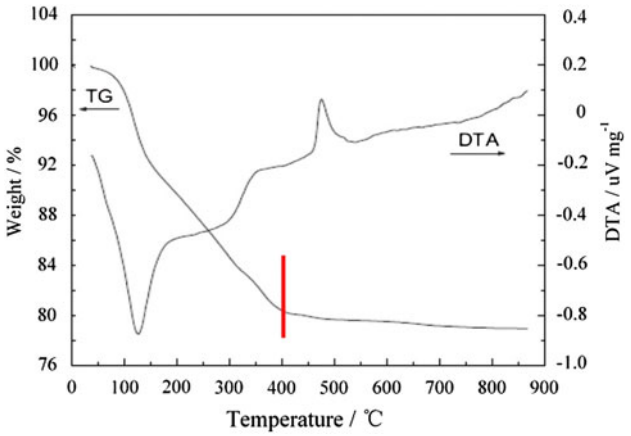

Fig. 1 TG/DTA curves of amorphous $FePO_4{\cdot}2H_2O$

$FePO_4{\cdot}2H_2O$, which is consistent with an endothermic peak between 131 and 162 °C in the DTA curve. There is also a slow weight loss in the range of 162–400 °C, corresponding to the loss of another 1.0 mol of water from the compound [27]. At 485 °C, an exothermic peak, which is not accompanied by appreciable weight loss in the TG curve, appears in the DTA curve. This peak is likely related to the structural transformation of the $FePO_4$ framework [28]. Combining the TG results with the elemental analysis of the precipitate that gives a molar ratio of Fe:P = 1:1, the formulas $FePO_4{\cdot}2H_2O$ is obtained for the as-prepared compound.

Figure 2 shows the XRD patterns of as-prepared and heated $FePO_4$. The as-prepared $FePO_4{\cdot}2H_2O$ was found to be completely amorphous. After the amorphous sample was heated in air at 500 °C for 10 h, crystalline $FePO_4$ nanoparticles formed. All the strong diffraction peaks can be indexed to the anhydrous $FePO_4$ hexagonal phase (JCPDS no. 29-0715).

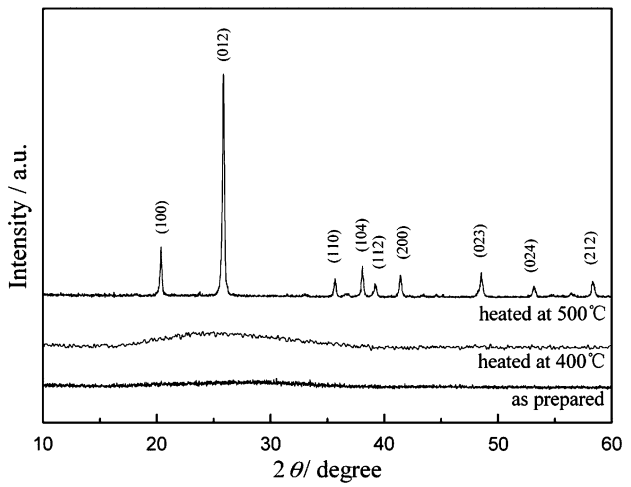

Fig. 2 XRD pattern of as prepared and heated $FePO_4{\cdot}2H_2O$

Figure 3 shows SEM micrographs of amorphous $FePO_4{\cdot}2H_2O$ synthesized at different temperatures by the co-precipitation method. The $FePO_4{\cdot}2H_2O$ particles in all the samples are uniform. The average diameter of the particles prepared at 0, 25, 50, and 75 °C are about 125, 90, 65, and 40 nm, respectively. The primary particle size was found to decrease gradually and become more uniform with increasing reaction temperature. This principle can be explained from two aspects [22]. (1) More crystal nucleuses are formed at higher temperature, thus consuming more reactants at the initial stage, which leads to the formation of finer particles. (2) At elevated temperature, the activating molecules move faster, increasing the collision rate and collision efficiency between anions and cations. Smaller nanoparticles form when the rate of nucleation formation is higher than that of grain growth. Accordingly, the size-controllable $FePO_4{\cdot}2H_2O$ provides series of uniform precursors for the next lithiation procedure.

The amorphous $FePO_4$ (after annealing at 400 °C) was lithiated to form amorphous $LiFePO_4$ by using LiI as the reducing agent. The lithiated sample was then calcined at 700 °C for 2 h under reducing atmosphere after mixed with sucrose. The chemical analysis of the lithiated compound was tested by flame and graphite atomic absorption spectrometries (Varian 220FS), it showed that the molar ratio of Li:Fe:P was 1:1:1, respectively, thus suggesting that the amorphous $FePO_4$ was completely lithiated.

Figure 4 shows the XRD patterns of the $LiFePO_4$/C composites after calcination. All samples exhibit a single phase $LiFePO_4$ with ordered olivine structure (JCPDS no. 40-1499). The amount of carbon in the $LiFePO_4$/C composite was about 6 wt% measured by leaching out from hydrochloric acid solution [10]. However, there are no diffraction peaks of carbon, possibly due to the presence of amorphous carbon. The diffraction peaks became slightly sharper with decreasing the synthesizing temperature of the $FePO_4$ precursor, which is in accordance with the particle size of the final products based on the Scherrer equation.

The SEM micrographs of the $LiFePO_4$/C composites are shown in Fig. 5. Compared with Fig. 3, it is easy to find that $LiFePO_4$/C composites completely maintained the shape and size of the precursor $FePO_4{\cdot}2H_2O$, suggesting that the $FePO_4$ precursor serves as a core for forming ultrafine and sphere-like $LiFePO_4$ particles. Meanwhile, no grain growth was observed during the chemical lithiation and calcination even without using any surfactant. Because of short reaction time and mild reaction conditions, the $LiFePO_4$/C can maintain the morphology and size of amorphous $FePO_4{\cdot}2H_2O$. Therefore, size-controllable $LiFePO_4$/C composite can be obtained by controlling the formation of $FePO_4{\cdot}2H_2O$ precursor.

To evaluate the rate capability of the $LiFePO_4$/C, the samples were charged to 4.2 V at the same current of 0.2 C

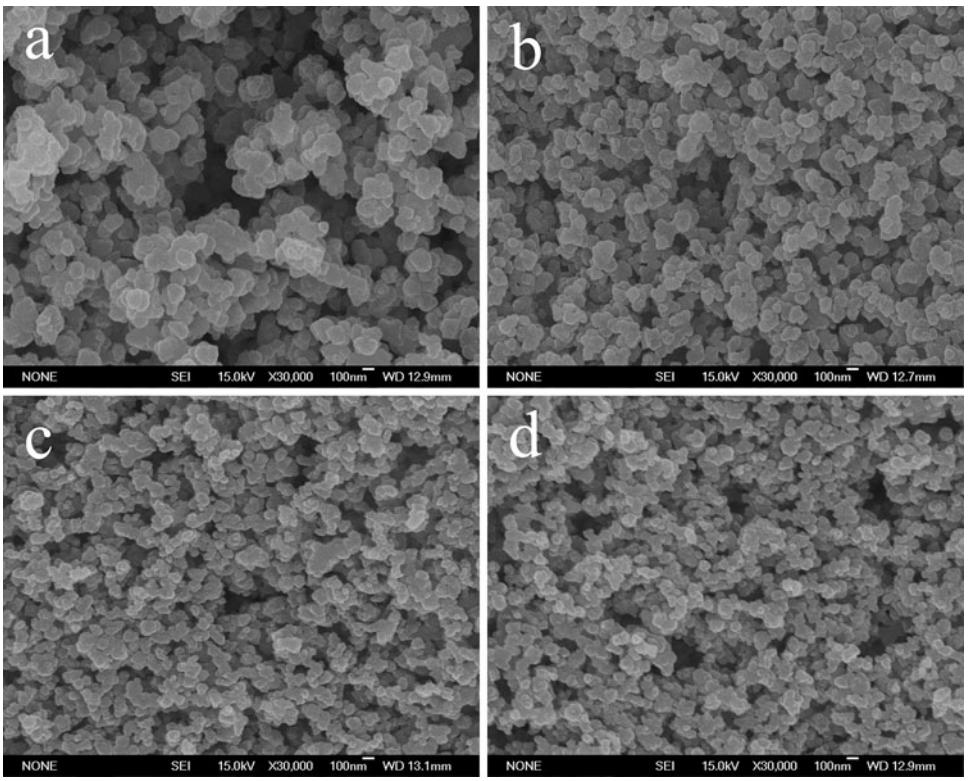

Fig. 3 SEM micrographs of amorphous $FePO_4{\cdot}2H_2O$ synthesized at different temperatures (**a** 0 °C, **b** 25 °C, **c** 50 °C, **d** 75 °C)

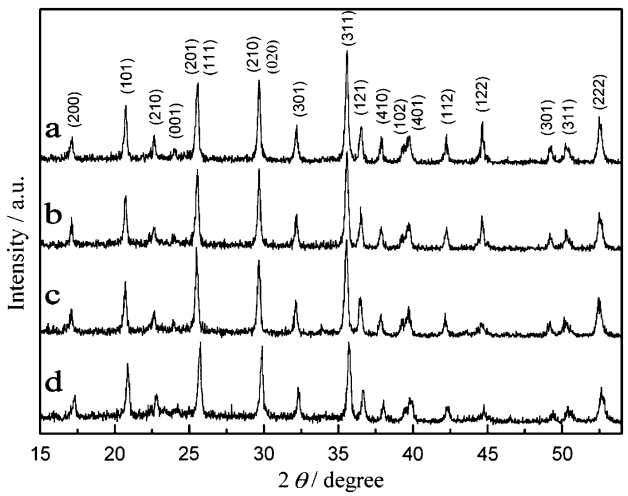

Fig. 4 XRD patterns of $LiFePO_4$/C obtained from $FePO_4{\cdot}2H_2O$ precursors synthesized at different temperatures (**a** 0 °C, **b** 25 °C, **c** 50 °C, **d** 75 °C)

and discharged to 2.5 V at different rates ranging from 0.1 to 5 C (i.e., from 17 to 850 mA g^{-1}). Figure 6 shows plots of the discharge capacity as a function of discharging rate for each sample. All $LiFePO_4$/C composites deliver almost the same specific capacity about 151.8 mAh g^{-1} at low discharge current (0.1 C rate). However, the $LiFePO_4$/C obtained from the precursor $FePO_4{\cdot}2H_2O$ synthesized at 75 °C shows better discharge rate performance. When increasing the current density to 170 mA g^{-1} (1 C rate), the sample shows its capacity about 133.5 mAh g^{-1}. Even at a rate as high as 5 C, the delivered capacity was still as high as 112.7 mAh g^{-1}. The $LiFePO_4$/C composites prepared by us show higher rate capability compared with $LiFePO_4$/C composites using iron phosphate synthesized by traditional solid-state methods [17, 18, 29]. The better performance in discharge capacity and rate capability can be attributed to the better dispersion of nanosized particles and in situ carbon coating on the surface of $LiFePO_4$ crystallites (as shown in the inset TEM images of Fig. 6).

Figure 7 shows the cycle performance of the prepared samples during continuous cycling at a current density of 85 mA g^{-1} (0.5 C). The specific capacity decreased slowly upon cycling for all the samples. The capacity fade of $LiFePO_4$/C composite was evaluated to be about 0.183, 0.140, 0.104, and 0.075 % per cycle, corresponding to the $FePO_4{\cdot}2H_2O$ precursors synthesized at 0, 25, 50, and 75 °C, respectively.

Figure 8a shows the discharge curves of $LiFePO_4$/C obtained from $FePO_4{\cdot}2H_2O$ precursor synthesized at 75 °C. The sample has a flat 3.4-voltage plateau at a high

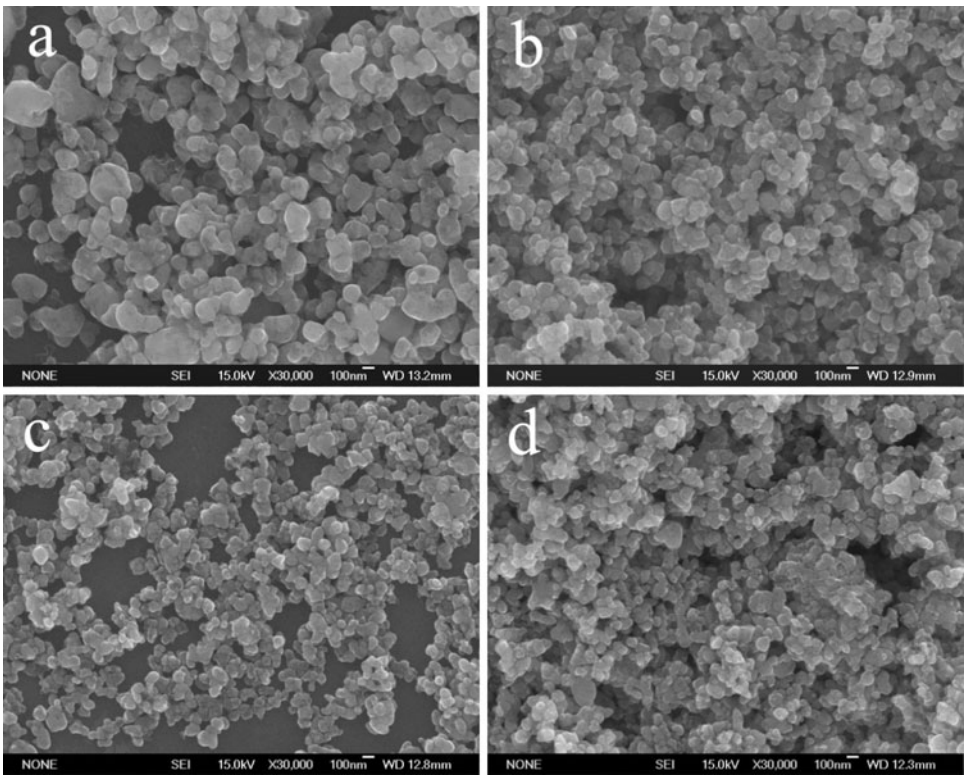

Fig. 5 SEM micrographs of $LiFePO_4$/C obtained from different $FePO_4 \cdot 2H_2O$ precursors (**a** 0 °C, **b** 25 °C, **c** 50 °C, **d** 75 °C)

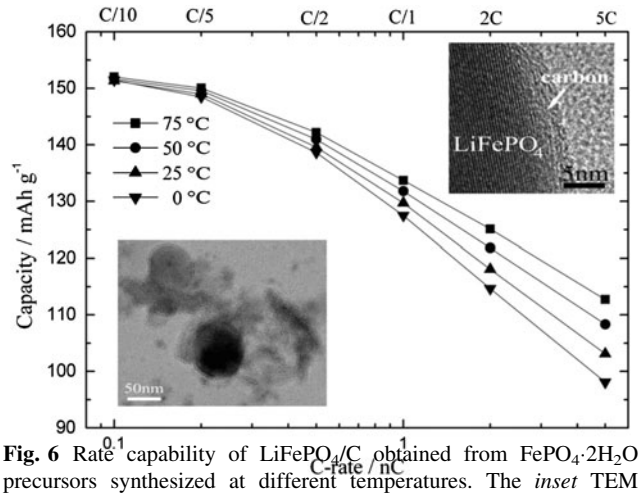

Fig. 6 Rate capability of $LiFePO_4$/C obtained from $FePO_4 \cdot 2H_2O$ precursors synthesized at different temperatures. The *inset* TEM images show the carbon morphology of the $LiFePO_4$/C composite

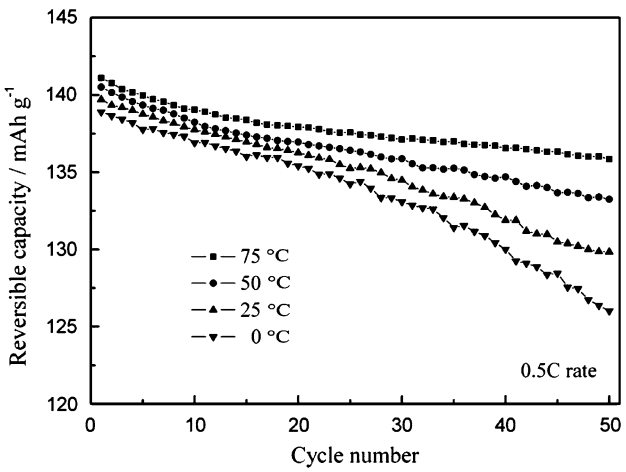

Fig. 7 Cycle performances at 0.5 C rate of $LiFePO_4$/C obtained from $FePO_4 \cdot 2H_2O$ precursors synthesized at different temperatures

discharge rate of 1 C. As the discharge current continued to increase, the drop of voltage plateau was not obvious, suggesting that the sample has better high rate discharge performance. The excellent cycling performance of the $LiFePO_4$/C composite is also supported by the CV curves, as shown in Fig. 8b. After "activation" in the first cycle, the current peaks of the following cycles become larger and narrower. The good overlap of the second and third cycles indicates that electrochemical reversibility is stably established. The better electrochemical performance of the material is attributed to its smaller particles, which reduce the diffusion length of lithium ions in $LiFePO_4$ and facilitate extraction and insertion of lithium ions [30].

4 Conclusions

Amorphous $FePO_4$ with controllable size was synthesized by co-precipitation method at different temperatures.

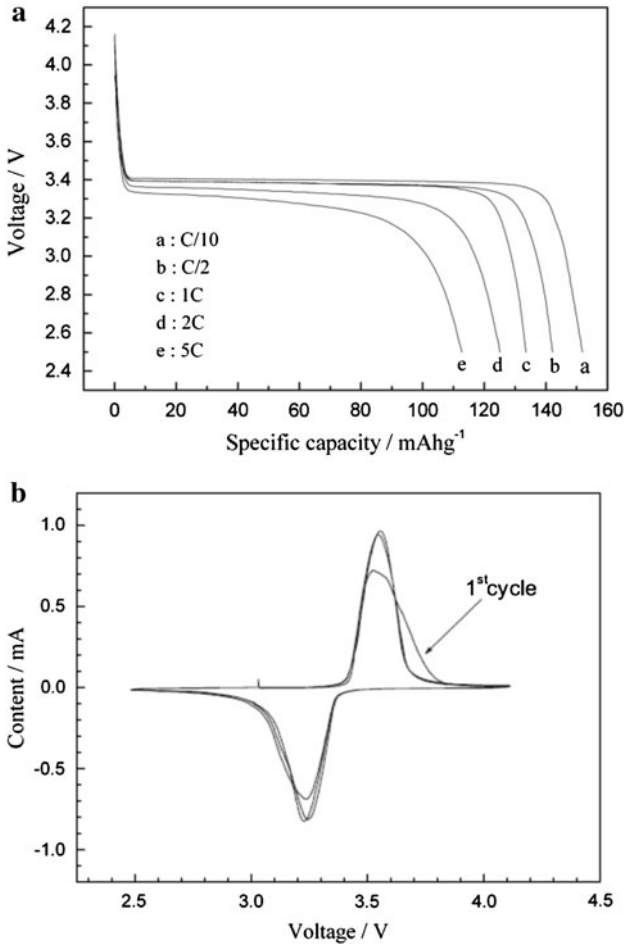

Fig. 8 The discharge curves (**a**) and cyclic voltammogram at a scan rate of 0.1 mV s^{-1} (**b**) of $LiFePO_4$/C obtained from $FePO_4 \cdot 2H_2O$ precursor synthesized at 75 °C

Nanocrystalline $LiFePO_4$/C was synthesized by the lithiation of the precursor with LiI and carbon coating with sucrose as the carbon source. The $LiFePO_4$/C composite obtained from the precursor $FePO_4 \cdot 2H_2O$ synthesized at 75 °C exhibits a specific capacity of 151.8 and 133.5 mAh g^{-1} at 0.1 and 1 C rate, with a low capacity fading of about 0.075 % per cycle over 50 cycles at 0.5 C rate. Chemical lithiation with LiI as a reducing agent and acetonitrile as a solvent is a useful method not only for converting $FePO_4$ to $LiFePO_4$, but also for obtaining nano-sized $LiFePO_4$ with various novel structures. The simple and effective method can be extended to the preparation of other lithium cathode materials such as $LiMn_2O_4$, $LiMnO_2$, $LiMnPO_4$, and $Li_4Ti_5O_{12}$.

Acknowledgments This study was supported by the Natural Science Foundation of China (11275121, 21241002), Science and Technology Committee of Shanghai (11DZ110020, 10ZR1411300), and Shanghai Leading Academic Disciplines Project (S30109).

References

1. Padhi AK, Nanjundaswamy KS, Goodenough JB (1997) Phospho-olivines as positive-electrode materials for rechargeable lithium batteries. J Electrochem Soc 144:1188–1194
2. Ellis B, Herle PS, Rho Y-H, Nazar LF, Dunlap R, Perry LK, Ryan DH (2007) Nanostructured materials for lithium-ion batteries: surface conductivity vs. bulk ion/electron transport. Faraday Discuss 134:119–141
3. Padhi AK, Nanjundaswamy KS, Masquelier C, Okada S, Goodenough JB (1997) Effect of structure on the Fe^{3+}/Fe^{2+} redox couple in iron phosphates. J Electrochem Soc 144:1609–1613
4. Meethong N, Kao Y-H, Speakman SA, Chiang Y-M (2009) Aliovalent substitutions in olivine lithium iron phosphate and impact on structure and properties. Adv Funct Mater 19: 1060–1070
5. Muraliganth T, Manthiram A (2010) Understanding the shifts in the redox potentials of olivine $LiM_{1-y}M_yPO_4$ (M = Fe, Mn, Co, and Mg) solid solution cathodes. J Phys Chem C 114: 15530–15540
6. Sun CS, Zhou Z, Xu ZG, Wang DG, Wei JP, Bian XK, Yan J (2009) Improved high-rate charge/discharge performances of $LiFePO_4$/C via V-doping. J Power Sources 193:841–845
7. Chang ZR, Lv HJ, Tang HW, Li HJ, Yuan XZ, Wang H (2009) Synthesis and characterization of high-density $LiFePO_4$/C compositions as cathode materials for lithium-ion batteries. Electrochim Acta 54:4595–4599
8. Su L, Jing Y, Zhou Z (2011) Li ion battery materials with core–shell nanostructures. Nanoscale 3:3967–3983
9. Sun CS, Zhang Y, Zhang XJ, Zhou Z (2010) Structural and electrochemical properties of Cl-doped $LiFePO_4$/C. J Power Sources 195:3680–3683
10. Prosini PP, Lisi M, Zane D, Paspuali M (2002) Determination of the chemical diffusion coefficient of lithium in $LiFePO_4$. Solid State Ion 148:45–51
11. Zhao B, Jiang Y, Zhang HJ, Tao HH, Zhong MY, Jiao Z (2009) Morphology and electrical properties of carbon $LiFePO_4$ cathode materials. J Power Sources 189:462–466
12. Ding Y, Jiang Y, Xu F, Yin J, Ren H, Zhuo Q, Long Z, Zhang P (2010) Preparation of nano-structured $LiFePO_4$/graphene composites by co-precipitation method. Electrochem Commun 12: 10–13
13. Lim S, Yoon CS, Cho J (2008) Synthesis of nanowire and hollow $LiFePO_4$ cathodes for high-performance lithium batteries. Chem Mater 20:4560–4564
14. Dominko R, Bele M, Gaberscek M, Remskar M, Hanzel D, Pejovnik S, Jamnik J (2005) Impact of the carbon coating thickness on the electrochemical performance of $LiFePO_4$/C composites. J Electrochem Soc 152:A607–A610
15. Wang XJ, Ren JX, Li YZ, Wei JP, Gao XP, Yan J (2005) Synthesis of cathode material "carbon-included" $LiFePO_4$ by microwave heating. J Inorg Chem 21:249–252
16. Wang M, Yang Y, Zhang YX (2011) Synthesis of micro-nano hierarchical structured $LiFePO_4$/C composite with both superior high-rate performance and high tap density. Nanoscale 3: 4434–4439
17. Mi CH, Zhao XB, Cao GS, Tu JP (2005) In situ synthesis and properties of carbon-coated $LiFePO_4$ as Li-ion battery cathodes. J Electrochem Soc 152:A483–A487
18. Prosini PP, Lisi M, Scaccia S, Carewska M, Cardellini F, Pasquali M (2002) Synthesis and characterization of amorphous hydrated $FePO_4$ and its electrode performance in lithium batteries. J Electrochem Soc 149:A297–A301
19. Andersson AS, Thomas JO (2001) The source of first-cycle capacity loss in $LiFePO_4$. J Power Sources 97–98:498–502

20. Wang GX, Liu H, Liu J, Qiao S, Lu GM, Munroe P, Ahn H (2010) Mesoporous $LiFePO_4$/C nanocomposite cathode materials for high power lithium ion batteries with superior performance. Adv Mater 22:4944–4948
21. Wang YG, Wang YR, Hosono E, Wang KX, Zhou HS (2008) The design of a $LiFePO_4$/carbon nanocomposite with a core-shell structure and its synthesis by an in situ polymerization restriction method. Angew Chem Int Ed 47:7461–7465
22. Huang YH, Ren HB, Peng ZH, Zhou YH (2009) Synthesis of $LiFePO_4$/carbon composite from nano-$FePO_4$ by a novel stearic acid assisted rheological phase method. Electrochim Acta 55: 311–315
23. Nien YH, Carey JR, Chen JS (2009) Physical and electrochemical properties of $LiFePO_4$/C composite cathode prepared from various polymer-containing precursors. J Power Sources 193: 822–827
24. Luo JY, Li XL, Xia YY (2007) Synthesis of highly crystalline spinel $LiMn_2O_4$ by a soft chemical route and its electrochemical performance. Electrochim Acta 52:4525–4531
25. Hwang SJ, Park DH, Kwon CW, Campet G, Choy JH (2004) Effect of reaction media on electrochemical performance of nanocrystalline manganese oxyiodides prepared by chimie douce route. J Power Sources 125:119–123
26. Kuo HT, Chan TS, Bagkar NC, Liu RS, Shen CH, Shy DS, Xing XK, Lee JF (2009) Effect of LiI amount to enhance the electrochemical performance of carbon-coated $LiFePO_4$. Electrochem Solid State Lett 12:A111–A114
27. Scaccia S, Carewska M, Bartolomeo AD, Prosini PP (2002) Thermoanalytical investigation of iron phosphate obtained by spontaneous precipitation from aqueous solutions. Thermochim Acta 383:145–152
28. Rajic N, Gabrovsek R, Kaucic V (2000) Thermal investigation of two FePO materials prepared in the presence of 1,2-diaminoethane. Thermochim Acta 359:119–122
29. Wang DY, Li H, Wang ZX, Wu XD, Sun YC, Huang XJ, Chen LQ (2004) New solid-state synthesis routine and mechanism for $LiFePO_4$ using LiF as lithium precursor. J Solid State Chem 177:4582–4587
30. Wang L, Huang Y, Jiang R, Jia D (2007) Preparation and characterization of nano-sized $LiFePO_4$ by low heating solid-state coordination method and microwave heating. Electrochim Acta 52:6778–6783